Synthetic Biodegradable Aliphatic Polyester/ Montmorillonite Nanocomposites

Sung T. Lim, Yang H. Hyun, and Hyoung J. Choi*

Department of Polymer Science and Engineering, Inha University, Incheon 402-751, Korea

Myung S. Jhon

Department of Chemical Engineering, Carnegie Mellon University, Pittsburgh, Pennsylvania 15213-3890

Received November 12, 2001. Revised Manuscript Received February 11, 2002

Biodegradable aliphatic polyesters (BAPs), synthesized from diols and dicarboxylic acids, and organophilic montmorillonite (OMMT) were intercalated by a solvent-casting method using chloroform as a cosolvent to produce nanocomposite (BAP/OMMT). The *d* spacings of both BAP and BAP/OMMT were examined by X-ray diffraction analysis, and the microstructure of BAP/OMMT was examined by transmission electron microscopy. Melting temperature changes and residuals were measured by thermal gravimetric analysis. Tensile strength and elongation were also examined with a universal testing machine. Increases in both the thermal stability and the mechanical strength of BAP/OMMT were observed for several different OMMT loadings. The rheological properties of the BAP/OMMTs were also examined with a rotational rheometer having a parallel-plate geometry. The shear viscosity at low shear rate exhibited a Newtonian plateau even at high loading and showed a higher degree of shear thinning at higher shear rate. Both the Newtonian plateau and the enhanced power-law behavior were correlated with a scaling function.

Introduction

Currently, there is considerable interest in biodegradable polymers, which can be used as alternatives to plastics, thus reducing the pollution caused by plastic wastes, and as renewable resources for polymer manufacturing.[1] Synthetic polymers are generally advantageous (e.g., have a well-balanced supply, a low cost, and excellent processibility) in the processing of commodity polymers ranging from inexpensive daily necessities to expensive specialty composites, including advanced medical materials. However, these polymers, which are generally obtained from the petrochemical products, have low recovery and reproduction rates and are nonbiodegradable. As a result, various biodegradable polymers have been investigated,[2] including poly(hydroxybutyrate) (PHB),[3] pullulan, chitosan derivatives, polyglycolide, and polylactide.[4] Of these, focus has centered on a bacterial aliphatic PHB[5,6] and its copolymers produced by various types of microorganisms. Unfortunately, this polymer has limited practical applications because of its high production costs, narrow processibility window, and relatively low impact resistance.

Biodegradable aliphatic polyesters (BAPs), which are usually synthesized from a diol and dicarboxylic acid through a condensation polymerization,[7] are considered to be the most promising biodegradable plastics because of their low production costs and easy processibility in large-scale production. BAPs are excellent packaging materials, substantially reducing environmental pollution. Difficulties are encountered, however, in their practical application because of their low melting temperature and poor thermal stability. Even though BAPs are comparable to PHB in terms of cost and capabilities, their higher cost compared to conventional plastics limits their use.

End users determine the desirable properties of these resins. In beverage bottle applications, for example, water and alcohol permeability and carbon dioxide barrier properties are dictating factors. On the other hand, for agricultural and construction applications, soil biodegradability is the dictating factor.[7] For each of these purposes, blends of BAP with various polymers, including linear low-density polyethylene,[8] poly(epichlorohydrin),[9] starch,[10] and poly(vinyl acetate),[11] have been examined.

* Corresponding author. Telephone: (82)-32-860-7486. Fax: (82)-32-865-5178. E-mail: hjchoi@inha.ac.kr.

(1) Ikada, Y.; Tsuji, H. *Macromol. Rapid Commun.* **2000**, *21*, 117.
(2) Avella, M.; Martuscelli, E.; Raimo, M. *J. Mater. Sci.* **2000**, *35*, 523.
(3) Choi, H. J.; Kim, J. H.; Kim, J. *Macromol. Symp.* **1997**, *119*, 149.
(4) Cooper-White, J. J.; Mackay, M. E. *J. Polym. Sci. B: Polym. Phys.* **1999**, *37*, 1803.
(5) Choe, S.; Cha, Y. J.; Lee, H. S.; Yoon, J. S.; Choi, H. J. *Polymer* **1995**, *36*, 4977.
(6) Park, S. H.; Choi, H. J.; Lim, S. T.; Shin, T. K.; Jhon, M. S. *Polymer* **2001**, *42*, 5737.
(7) Fujimaki, T. *Polym. Degrad. Stab.* **1998**, *59*, 209.
(8) Kim, J.; Kim, J. H.; Shin, T. K.; Choi, H. J.; Jhon, M. S. *Eur. Polym. J.* **2001**, *37*, 2131.
(9) Kim, J.; Shin, T. K.; Choi, H. J.; Jhon, M. S. *Polymer* **1999**, *40*, 6873.
(10) Ratto, J. A.; Stenhouse, P. J.; Auerbach, M.; Mitchell, J.; Farrell, R. *Polymer* **1999**, *40*, 6777.

10.1021/cm010377j CCC: $22.00
Published on Web 03/09/2002

Recently, polymer/clay nanocomposites (P/CNs) have attracted considerable interest because of their ability to control the dispersion quality of clay particles in polymer matrixes at the nanoscopic level.[12,13] Layered clay (or silicate) acting as a nanofiller in a polymer matrix can be used as a nanocomposite reinforcement material.[14−16] The mixing of polymers filled with layered silicate produces microstructural blends different from conventional dispersions of inorganic fillers.[17] P/CNs exhibit increased moduli,[18] reduced gas permeability,[19] enhanced thermal stability, and self-extinguishing fire-retardant characteristics.[20,21] For example, a doubling of the tensile modulus and an increasing of the heat distortion temperature by 100 °C can be achieved for nylon/clay nanocomposites with as little as 2 vol % of inorganic content.[22] The improved performance depends primarily on the distribution, arrangement, and interfacial bonding between the clay layers and the polymers.[23] Recently, P/CNs prepared by emulsion polymerization with polyaniline (PANI)[24,25] and styrene−acrylonitrile copolymer[26] have been used as suspended particles in dry-base electrorheological fluids on account of their tunable rheological properties.[27] PANI/clay nanocomposites can also be used in other applications, including corrosion protection and enhanced electrical conductivity.[28,29]

The mechanical and rheological properties of P/CNs are directly related to nanocomposite microstructure and are of vital importance to processing technology. Despite their apparent importance, the effects of intercalated/exfoliated structures and surface characteristics of the polymers and layered silicates on the rheological properties have yet to be thoroughly investigated.[30] In this study, therefore, we undertake an investigation of these mechanical and rheological properties by preparing BAP-based nanocomposites with organophilic montmorillonite (OMMT). The introduction of BAP into nanocomposites, we believe, can substantially reduce the cost of biodegradable polymers.

Experimental Section

Sample Preparation. The BAP chains are intercalated into the layered silicates by a solvent-casting method with chloroform as a cosolvent. The BAP used (Skygreen 2109) was acquired from Sunkyong Industry in Korea. The BAP samples are copolymers synthesized from diols (1,4-butanediol and ethylene glycol) and dicarboxilic acids (succinic acid and adipic acid) with a weight-average molecular weight of 6.0×10^4 g/mol. Commercially available OMMT (Cloisite 25A), produced by Southern Clay Products (Gonzales, TX), was used for the layered silicate. The pristine Na^+-montmorillonite (MMT) was converted into the organophilic clay by a cation-exchange reaction with dimethyl hydrogenated tallow (2-ethylhexyl) quaternary ammonium methyl sulfate with a MMT cationic-exchange capacity of 95 mequiv/100 g. Different amounts of BAP were dissolved, and OMMT was dispersed in chloroform for 48 h. The chloroform was evaporated, and all of the samples were then dried in a vacuum oven for 24 h. Samples were then formed into a disk-shaped film with a thickness of 2.18 mm and a diameter of 18 mm using a hot press (Carver, model 3852, Wabash, IN) at 140 °C for rheological testing. We set the temperature and pressure at 140 °C and 13.6 MPa, respectively. The molding temperature (140 °C) is not much higher than the melting temperatures (T_m's) of the samples (the T_m's are 90 °C for BAP and 110 °C for BAP/OMMT from differential scanning calorimetry), but it is significantly lower than the thermal decomposition temperatures of the nanocomposite systems. A 13.6 MPa pressure was applied to the samples for less than 2 min, before the samples were cooled to the ambient pressure. Vaia et al.[31] demonstrated the static melt intercalation method with polystyrene (PS) and organically modified silicate hybrids at a much higher pressure of 70 MPa (without imposed shear). These samples were then annealed in a vacuum at temperatures greater than the glass transition temperature (∼100 °C) of PS. The conditions in Vaia et al.[31] are more severe than our compression molding conditions, which were intended to avoid any changes in the originally prepared nanocomposite samples, thereby allowing the effect of compression molding on the solvent-casting nanocomposite system to be neglected.

Measurements. The insertion of BAP into the OMMT layers was confirmed by X-ray diffractometry (XRD). A Guinier focusing camera using a quartz crystal monochromator in a Philips PW-1847 X-ray crystallographic unit (40kV and 40mV) fitted with a copper target was used for recording data in the range of $2\theta = 1.5-30°$.

Transmission electron microscopy (TEM) images were obtained using a JEM 2000 EX-II instrument (JEOL, Tokyo, Japan) operated with 1×10^4 and 5×10^4 magnification at an accelerated voltage of 100 kV. All of the ultrathin sections (less than 3 μm) were microtomed using a Super NOVA 655001 instrument (Leica, Swiss) with a diamond knife and were then subjected to TEM observation without staining.

Thermal gravimetric analysis (TGA) was performed using PL-TGA (Polymer Laboratories, TGA 1000, Shropshire, U.K.) by increasing the temperature from 40 to 500 °C at a heating rate of 20 °C/min in a nitrogen atmosphere. A rotational rheometer (Physica, MCR 300, Stuttgart, Germany) with a parallel-plate geometry (25 mm diameter) was used for the rheological measurements. The shear viscosity in a molten state as a function of shear rate ($0.001-2\ s^{-1}$) at 140 °C was measured with a 1.1-mm gap distance between the parallel plates.

Further, for the measurement of mechanical properties, the premixed material was compression-molded into a sheet at 140 °C and 95.7 MPa in a heated press. The sheet was cut into rectangles with a thickness of 0.15 mm and width of 5.0 mm.

(11) Shin, T. K.; Kim, J.; Choi, H. J.; Jhon, M. S. *J. Appl. Polym. Sci.* **2000**, *77*, 1348.
(12) Alexandre, M.; Beyer, G.; Henrist, C.; Cloots, R.; Rulmant, A.; Jerome, R.; Dubois, P. *Macromol. Rapid Commun.* **2001**, *22*, 643.
(13) Strawhecker, K. E.; Manias, E. *Chem. Mater.* **2000**, *12*, 2943.
(14) Alexandre, M.; Dubois, P. *Mater. Sci. Eng.* **2000**, *R28*, 1.
(15) LeBaron, P. C.; Pinnavaia, T. J. *Chem. Mater.* **2001**, *13*, 3760.
(16) Rong, J.; Jing, Z.; Li, H.; Sheng, M. *Macromol. Rapid Commun.* **2001**, *22*, 329.
(17) Zanetti, M.; Lomakin, S.; Camino, G. *Macromol. Mater. Eng.* **2000**, *279*, 1.
(18) Wang, Z.; Pinnavaia, T. J. *Chem. Mater.* **1998**, *10*, 3769.
(19) Messersmith, P. B.; Giannelis, E. P. *J. Polym. Sci. A: Polym. Chem.* **1995**, *33*, 1047.
(20) Dietsche, F.; Mülhaupt, R. *Polym. Bull.* **1999**, *43*, 395.
(21) Zhu, J.; Morgan, A. B.; Lamelas, F. J.; Wilkie, C. A. *Chem. Mater.* **2001**, *13*, 3774.
(22) Usuki, A.; Kawasumi, M.; Kojima, Y.; Okada, A.; Kurauchi, T.; Kamigaito, O. *J. Mater. Res.* **1994**, *8*, 1174.
(23) Huang, J. C.; Zhu, Z. K.; Yin, J.; Qian, X. F.; Sun, Y. Y. *Polymer* **2001**, *42*, 873.
(24) Kim, J. W.; Kim, S. G.; Choi, H. J.; Jhon, M. S. *Macromol. Rapid Commun.* **1999**, *20*, 450.
(25) Kim, J. W.; Kim, S. G.; Choi, H. J.; Suh, M. S.; Shin, M. J.; Jhon, M. S. *Int. J. Mod. Phys. B* **2001**, *15*, 657.
(26) Kim, J. W.; Noh, M. H.; Choi, H. J.; Lee, D. C.; Jhon, M. S. *Polymer* **2000**, *41*, 1229.
(27) Sim, I. S.; Kim, J. W.; Choi, H. J.; Kim, C. A.; Jhon, M. S. *Chem. Mater.* **2001**, *13*, 1243.
(28) Yeh, J. M.; Liou, S. J.,; Lai, C. Y.; Wu, P. C. *Chem. Mater.* **2001**, *13*, 1131.
(29) Kim, B. H.; Jung, J. H.; Kim, J. W.; Choi, H. J.; Joo, J. *Synth. Met.* **2001**, *117*, 115.
(30) Hoffmann, B.; Dietrich, C.; Thomann, R.; Friedrich, C.; Mülhaupt, R. *Macromol. Rapid Commun.* **2000**, *21*, 57.
(31) Vaia, R. A.; Jandt, K. D.; Kramer, E. J.; Giannelis, E. P. *Chem. Mater.* **1996**, *8*, 2628.

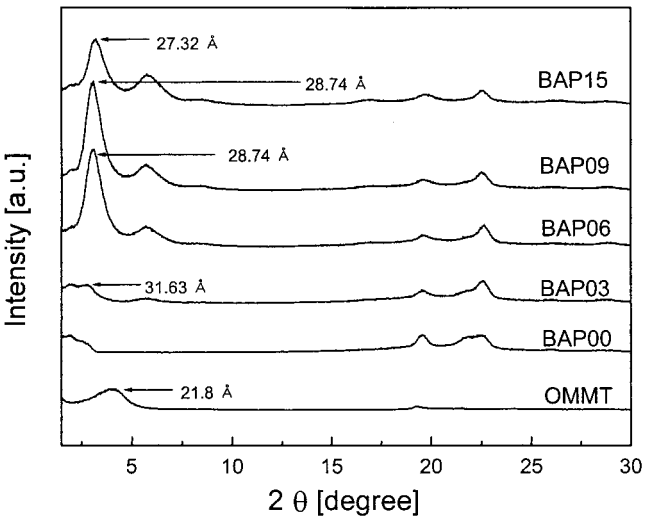

Figure 1. X-ray diffraction patterns of BAP/OMMT nanocomposites and OMMT.

A universal testing machine (Hounsfield, H25KS Chamber System, Surrey, U.K.) was used to measure both the tensile modulus and the elongation at break with a speed of 10.0 mm/min for a sample length of 30.0 mm at 25 °C.

Results and Discussion

Figure 1 shows the XRD results for the series pure BAP, BAP/OMMT, and OMMT. The BAP-to-OMMT ratios used in our study were 100/0, 97/3, 94/6, 91/9, and 85/15 by weight, with code names of BAP00 (pure BAP), BAP03, BAP06, BAP09, and BAP15, respectively. Each nanolayer of smectite clay (e.g., MMT) consisted of two tetrahedral sheets (mainly Si and occasionally Al) and a central octahedral sheet (occupied by Mg, Al, etc.), with a lateral dimension of 0.2−2 μm and a thickness of about 1 nm. The stacking of nanolayers forms tactoids (crystallines) that are typically 0.1−1 μm thick.[14] MMT exhibits a net negative charge on the lamellar surface, which enables it to adsorb cations, such as Na^+ or Ca^{2+}, and occupies the gallery space between nanolayers in the naturally occurring mineral. Because the negative charge originates in the silicate layer, the cationic headgroup of the alkylammonium molecule preferentially resides at the layer surface with the aliphatic tails being removed from the surface. The presence of these aliphatic chains in the galleries alters the original silicate surface from hydrophilic to organophilic. Additionally, the organic cations can contain various functional groups that react with the polymers and improve adhesion between the reinforcement particles and the matrix, thus producing nanocomposites with high dispersion in organic solvents. Natural Na^+-MMT has also been extensively used for nanocomposites via the emulsion polymerization method.[24]

The intercalation of polymer chains usually increases the interlayer spacing relative to that of the pure clay, leading to a shift in the X-ray diffraction peak toward a lower angle. The parameters were calculated from the observed peaks of the angular position 2θ by the Bragg formula: $\lambda = 2d \sin \theta$. The finite layer expansion associated with intercalated structures resulted in a new basal reflection that corresponded to the layer gallery height of the intercalated nanocomposites. The d spacing of the original OMMT expanded from 2.18 to 3.16 nm for BAP03. However, when the amount of OMMT was increased beyond 6 wt %, no change in d spacing (2.73 nm for BAP15) was observed. We further observed that the intensity of the XRD peak progressively decreased with increasing clay loading. The increase in d spacing to 2.73 nm (for BAP15) compared to the 2.18 nm of the original OMMT indicates a partial insertion of BAP segments in the interlayers of the OMMT. Such intercalation of BAP into the layers of C25A has previously been observed indirectly by either dielectric spectroscopy[32] or conductivity measurements.[33] In the case of intercalated PANI/Na^+-MMT, Kim et al.[33] found that the clay layers interrupted the delocalization of charge carriers, weakening the interchain interactions and producing a greater state of disorder and lower conductivity according to dc electrical conductivity measurements.

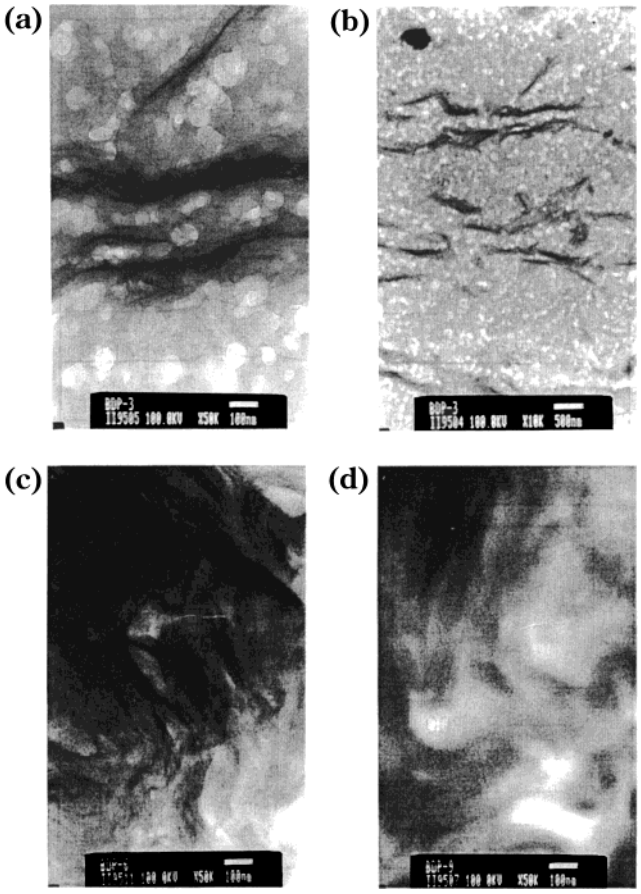

Figure 2. Different TEM images of BAP/OMMT nanocomposites: (a) BAP03 (×50 000, 100-nm scale), (b) BAP03 (×10 000, 500-nm scale), (c) BAP06 (×50 000, 100-nm scale), and (d) BAP09 (×50 000, 100-nm scale)

In addition to XRD, to validate the morphology of the nanocomposites, the internal nanometer-scale structure was observed by TEM, which provides direct visualization of the morphology, atomic arrangement, spatial phase distribution, and structural effects of a selected sample area. Figure 2 shows the TEM images of the nanocomposites (a) BAP03 (×50 000), (b) BAP03 (×10 000), (c) BAP06 (×50 000), and (d) BAP09 (×50 000),

(32) Anastasiadis, S. H.; Karatasos, K.; Vlachos, G.; Manis, E.; Giannelis, E. P. *Phys. Rev. Lett.* **2000**, *84*, 915.

(33) Kim, B. H.; Jung J. H.; Hong, S. H.; Joo, J.; Epstein, A. J.; Mizoguchi, K.; Kim, J. W.; Choi, H. J. *Macromolecules* **2002**, *35*, 1419.

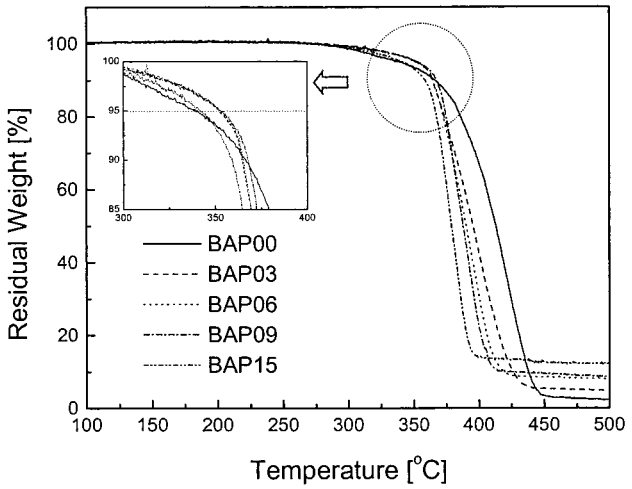

Figure 3. TGA of BAP/OMMT for several OMMT loadings.

where the dark entities are intercalated OMMT layers. From the TEM results, it is clear that the stacks of OMMT layers forming the clay crystallites are well dispersed in the polymer matrix. The TEM results further reveal multiple ordered platelets.[34] Accordingly, the dispersion of clay in the polymer matrix is conjectured to be related to platelets agglomerated into clay particles, not to individual clay platelets.

Figure 3 shows the TGA results for BAP00 and BAP/OMMT of several OMMT contents. We found an increase in the thermal degradation temperature and thermal degradation rate with an increasing amount of dispersed OMMT. With the exception of BAP15, the onset of thermal degradation for BAP/OMMT was improved by the addition of the clay. We designated the thermal degradation point as the temperature of 5% weight loss. This temperature increased more (approximately 15 °C) for BAP03, BAP06, and BAP09 than for BAP00 and BAP15. A small amount of clay increased the residual weight of BAP/OMMT because of the restricted thermal motion of the polymer in the silicate interlayers. The residual weight at 450 °C increased in the order BAP00 < BAP03 < BAP06 < BAP09 < BAP15. The silicate has an excellent barrier property that prevents against permeation of various atmospheric gases. The addition of clay enhanced the performance by acting as a superior insulator and mass-transport barrier to the volatile products generated during decomposition. This kind of improvement in thermal stability was also observed in other systems of SAN,[26] the intercalated nanocomposites prepared by emulsion polymerization.

The increase in degradation rate with increasing amount of dispersed clay observed in the TGA results is the main difference between our system and the previous results. The role of clay in the hybrid structure might be the reason for this difference. As mentioned before, the clay acts as a heat barrier, which could enhance the overall thermal stability of the system, as well as assisting in the formation of char after thermal decomposition. Thereby, in the beginning stage of thermal decomposition, the clay could shift the decomposition temperature higher. However, after that, this heat barrier effect would result in a reverse thermal stability. In other words, the P/CN domain could hold accumulated heat that could be used as a heat source to accelerate the decomposition process, in conjunction with the heat flow supplied by the outside heat source. Understanding this effect requires that one recal the intercalated tactoid structures shown in Figure 2. This explanation might not be valid with other systems, however. Therefore, it is difficult to explain the exact mechanism of this reverse trend, and further study is required.

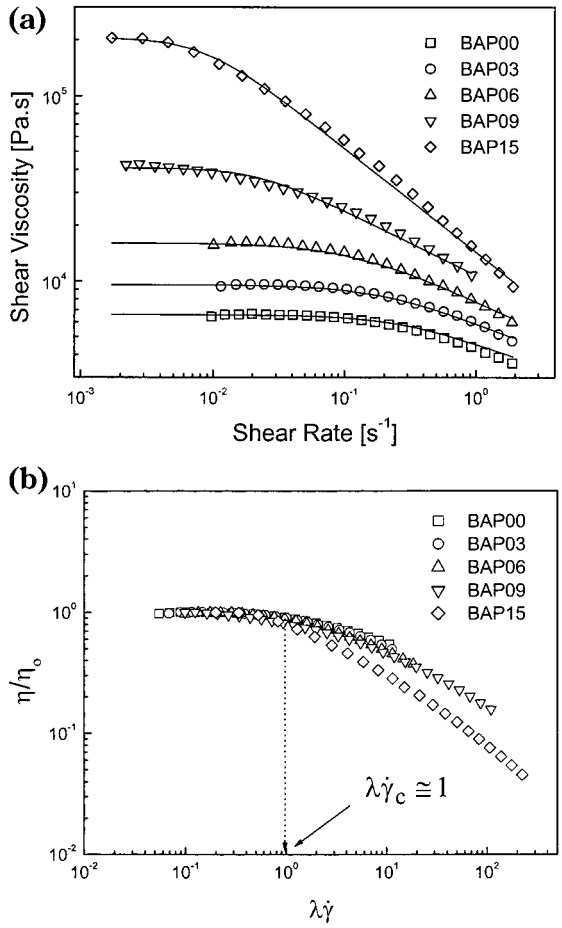

Figure 4. (a) Shear viscosity vs shear rate of BAP/OMMT for various OMMT loadings at 140 °C. Symbols represent the experimental data. Solid lines represent Carreau model (eq 1). (b) Scaled plot for η_0/η_0 vs $\lambda\dot{\gamma}$.

Figure 4 shows the shear viscosity as a function of shear rate for BAP/OMMT and BAP. The shear viscosity of the P/CN systems decreased with increasing shear rate (shear-thinning behavior).[35−38] The shear viscosity also increased substantially with OMMT content over a broad range of shear rates. At low shear rates, the shear viscosity data exhibited a Newtonian plateau even for high OMMT loadings. With increasing shear rate, the P/CNs exhibited higher degrees of shear-thinning behavior compared to the pure polymer systems. A similar trend was observed by Krishnamoorti et al.[39]

(34) Vaia, R. A.; Giannelis, E. P. *Macromolecules* **1997**, *30*, 8000.
(35) Choi, H. J.; Kim, S. K.; Hyun, Y. H.; Jhon, M. S. *Macromol. Rapid Commun.* **2001**, *22*, 320.
(36) Giannelis, E. P. *Appl. Organomet. Chem.* **1998**, *12*, 675.
(37) Choi, H. J.; Park, S. H.; Yoon, J. S.; Lee, H. S.; Choi, S. J. *Polym. Eng. Sci.* **1995**, *35*, 1636.
(38) Choi, H. J.; Kim, J.; Jhon, M. S. *Polymer* **1999**, *40*, 4135.
(39) Krishnamoorti, R.; Vaia, R. A.; Giannelis, E. P. *Chem. Mater.* **1996**, *8*, 1728.

Table 1. Carreau Model (Equation 1) Parameters Obtained for BAP/C N Systems

sample code	η_0 (Pa·s) × 10^{-4}	λ (s)	n
BAP00	0.66	5.69	0.76
BAP03	0.95	5.08	0.69
BAP06	1.60	9.49	0.67
BAP09	4.06	44.90	0.65
BAP15	20.54	115.89	0.44

for intercalated poly(dimethyldiphenyl siloxane)/OMMT nanocompsoites with several different silicate loadings. They observed that the shear viscosity of these nanocomposites increased monotonically with OMMT loading and that the intercalated nanocomposites displayed shear-thinning behavior at low shear rates [even though the viscosity of pure poly(dimethyldiphenyl siloxane) is shear-rate-independent].

The increase in shear viscosity of the P/CNs with increasing clay concentration was recently analyzed using a mean-field theroy.[40] Furthermore, in the case of intercalated polystyrene−polyisoprene block copolymer/MMT nanocomposite, Krishnamoorti et al.[41] observed that the steady shear viscosities for the nanocomposites exhibited enhanced shear-thinning behavior at low shear rates. In other words, the viscosity at high shear rates showed more decreased values from the zero-shear viscosities with increasing clay loading, and the values were almost identical to those of unfilled polymer. Although the exact mechanism that causes the shear-thinning behavior is not clear, it can be deduced that the orientation of the silicate layers under shear is the main cause. With increasing shear rate, the intercalated chain conformations change as the coils align parallel to the flow.[39] Nevertheless, because of this shear-thinning property, the nanocomposites can be processed in the melt state using the conventional equipment available in a manufacturing line.

To examine the relationship between shear viscosity (η) and shear rate ($\dot{\gamma}$), we fit the measured viscosity to the Carreau model,[42] given by

$$\eta = \frac{\eta_0}{[1 + (\dot{\gamma}\lambda)^2]^{(1-n)/2}} \qquad (1)$$

Here, η_0 is the zero-shear-rate viscosity, λ is a characteristic (or relaxation) time, and n is a dimensionless parameter, where the slope of η vs $\dot{\gamma}$ in the power-law region is given by $n - 1$. Note that, in the special case of $n = 1$ or $\dot{\gamma}\lambda \rightarrow 0$, eq 1 reduces to the Newtonian fluid model. For $n < 1$, eq 1 predicts shear-thinning behavior. From the calculated values of n, λ, and η_0 for our systems (Table 1), we found that the degree of shear thinning and λ increase with the OMMT loading. The degree of shear thinning increases with clay loading (Figure 4a) because of the alignment of clay layers under shear,[39,40] i.e., the suspension microstructure changes from a random orientation to a shear-induced ordered orientation.[35] Note that the Carreau model fits BAP/PVAc blends[11] and PEO/clay nanocomposites[35] very well. On the other hand, the shear viscosity of the intercalated polystyrene/Na^+-MMT nanocomposite was found to be fitted well by the Cross−Williamson model.[43]

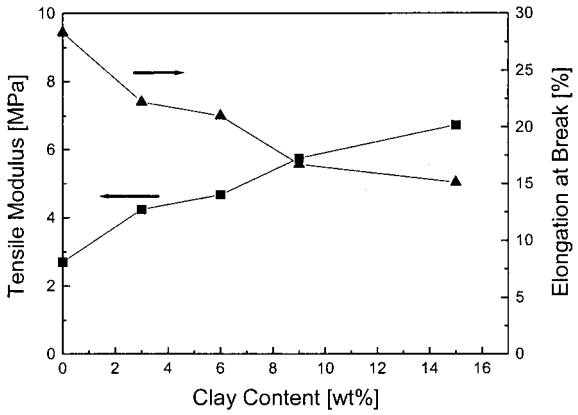

Figure 5. Tensile modulus and elongation at break vs OMMT loading.

The scaling curves (Figure 4b) demonstrate a Newtonian plateau at low shear rates and power-law behavior at high shear rates. A crossover from a Newtonian plateau to a shear-thinning region occurs at the critical shear rate $\dot{\gamma}_c$.[35,44] $\dot{\gamma}_c$ is approximately equal to the inverse of the characteristic time, which is the longest relaxation time required for the elastic structures. From the measured shear viscosities, we obtained the critical shear rate for each sample as 0.18, 0.12, 0.08, 0.02, and 0.007 s^{-1} for BAP00, BAP03, BAP06, BAP09, and BAP15, respectively. We found a correlation between λ (λ is given in Table 1), which is obtained from Carreau model, and $\dot{\gamma}_c$ for BAP/OMMT. We scaled the shear viscosity with respect to the zero-shear viscosity (η_0) and then plotted the result as a function of the product of λ and $\dot{\gamma}$, as shown in Figure 4b. We observed that, at $\lambda\dot{\gamma}_c \approx 1$, a departure from the plateau region begins. We postulate that $\lambda\dot{\gamma}_c$ is a universal constant with a value of 1, even though λ depends on the system (i.e., volume fraction, etc). The constant value $\lambda\dot{\gamma}_c \approx 1$ is illustrated in Figure 4b. A similar concept has also been used to describe the anomalous lateral migration of a rigid sphere in viscoelastic fluid flow.[45]

Polymer reinforcement with clay loading is illustrated by the tensile modulus (or Young's modulus) and the elongation at break vs clay loading (Figure 5). A considerable improvement in tensile modulus and a dramatic decrease in elongation at break are gained with an increase in OMMT content. The enhancement in the tensile modulus can be directly attributed to the reinforcement provided by the intercalation of BAP in OMMT galleries, as well as a fine dispersion of OMMT particles in the BAP matrix. However, the effect of nanocomposite formation on the elongation at break has yet to be carefully investigated. Recently, a reduction in elongation at break was also reported for dispersed thermoplastics.[46]

(40) Hyun, Y. H.; Lim, S. T.; Choi, H. J.; Jhon, M. S. *Macromolecules* **2001**, *34*, 8084.
(41) Krishnamoorti, R.; Ren, J.; Silva, A. S. *J. Chem. Phys.* **2001**, *114*, 4968.
(42) Carreau, P. J.; De Kee, D. C.; Chhabra, R. P. *Rheology of Polymeric Systems: Principles and Application*; Hanser Publishers: New York, 1997.
(43) Kim, T. H.; Jang, L. W.; Lee, D. C.; Choi, H. J.; Jhon, M. S. *Macromol. Rapid Commun.* **2002**, *23*, 191.
(44) Solomon, M. J.; Almusallam, A. S.; Seefeldt, K. F.; Somwangthanaroj, A.; Varadan, P. *Macromolecules* **2001**, *34*, 1864.
(45) Choi, H. J.; Prieve, D. C.; Jhon, M. S. *J. Rheol.* **1987**, *31*, 317.
(46) Sur, G. S.; Sun, H. L.; Hyu, S. G.; Mark, J. E. *Polymer* **2001**, *42*, 9783.

Conclusion

We prepared, for the first time, polymer/clay nancomposites with synthetic BAP and OMMT by a solvent-casting method, verified the BAP insertion into the layered silicate by XRD, and examined the microstructure by TEM. An increase in thermal stability of the BAP/OMMT was achieved with increasing OMMT content (when the clay content was less than 15 wt %). Furthermore, the mechanical strength of BAP/OMMT also increased substantially with increasing clay content. The shear viscosity of BAP/OMMT at a low shear rate showed a Newtonian plateau even at high loadings. At a high shear rate, these nanocomposites exhibited higher degrees of shear-thinning behavior compared to pure BAP. The shear viscosity, or zero-shear-rate viscosity, of BAP/OMMT increased with OMMT content as the clay particles resisted flowing. In contrast to pure BAP, BAP/OMMT exhibited more rapid shear-thinning behavior with increasing OMMT loading, because of the reorientation of the dispersed OMMT particles and the deformation of the polymer matrix. The shear viscosities for BAP/OMMT were well represented by the Carreau model. The Newtonian plateau and power-law behavior were represented in a scaled curve to identify the critical shear rate.

We found that BAP/OMMT nanocomposites have enhanced thermal, mechanical, and rheological properties.

Acknowledgment. This study was supported by research grants from the Korea Science and Engineering Foundation (KOSEF) through the Applied Rheology Center (ARC), an official KOSEF-created engineering research center (ERC) at Korea University, Seoul, South Korea.

CM010377J